

On material transport in Hiuchi-nada by means of the horizontal two-dimensional dispersion model

Toshiyuki AWAJI

(Department of Applied Science, Kochi Women's University, Kochi 780, Japan)

(昭和59年11月27日 受理)

Abstract: To investigate material transport and the role of dispersion due to the combined effect of vertical shear and vertical turbulent diffusivity in Hiuchi-nada in the central part of Seto Inland Sea, the observed horizontal distributions of salinity in summer and winter are analyzed numerically based on the horizontal two-dimensional dispersion model developed by Awaji and Kunishi (1983)¹⁾. As a result, the horizontal distribution of salinity in summer might be mainly governed by both advection due to a steady current and the dispersion due to a tidal current. Whereas the horizontal distribution of salinity in winter might be governed only by the dispersion far larger than that due to a tidal current. Therefore, it can be recognized that dispersion plays an important role on horizontal transport of matter (e. g. salinity) in summer and winter.

1. Introduction

Recently the preservation of marine environment in inland seas such as Hiuchi-nada has come to be social problems. It is important to understand the mechanism of material transport when taking steps to preserve inland sea water environments.

Dispersion models used for the studies of material transport so far ²⁾⁻⁴⁾ have been concerned with the analysis of material transport in regions such as estuaries where material distributions may be regarded as horizontally one-dimensional. As clearly shown by Imasato *et al.* (1978)⁵⁾, however, in most cases material distributions in inland seas are horizontally two-dimensional because of their characteristics of geometry. This indicates that it is not adequate to apply horizontal one-dimensional dispersion models to the problem concerning material transport in inland seas, and therefore the process of material transport in inland seas should be investigated using a horizontal two-dimensional dispersion model. Recently the horizontal two-dimensional dispersion model was developed by Awaji and Kunishi (1983)¹⁾, hereafter referred to as *AK*, where horizontal two-dimensional dispersion equation was derived and dispersion coefficient was formulated without specifying the velocity profile both horizontally and vertically.

In the present paper, the fundamental mechanism of material transport in Hiuchi-nada, which is one of the typical inland seas in Japan and is located in the central part of Seto Inland Sea, is studied based on observed distributions of salinity. First the features of the observed distributions of salinity in summer and winter are described. Next the horizontal distributions of the depth-averaged salinity in summer and winter are numerically analyzed by means of the horizontal two-dimensional dispersion model.

2. Observed distributions of salinity in Hiuchi-nada

The topography of Hiuchi-nada is shown in Fig. 1. Both horizontal length scales from

north to south and from east to west are about 50 km. The mean depth is about 20 m. Hiuchi-nada is connected with Aki-nada through some straits (e.g. Kurushima Strait and Mihara Strait) in the western part, and with Bisan-seto in the eastern part. In Aug. and Dec. 1972, the observations of salinity were carried out by Nansei Fisheries Research La-

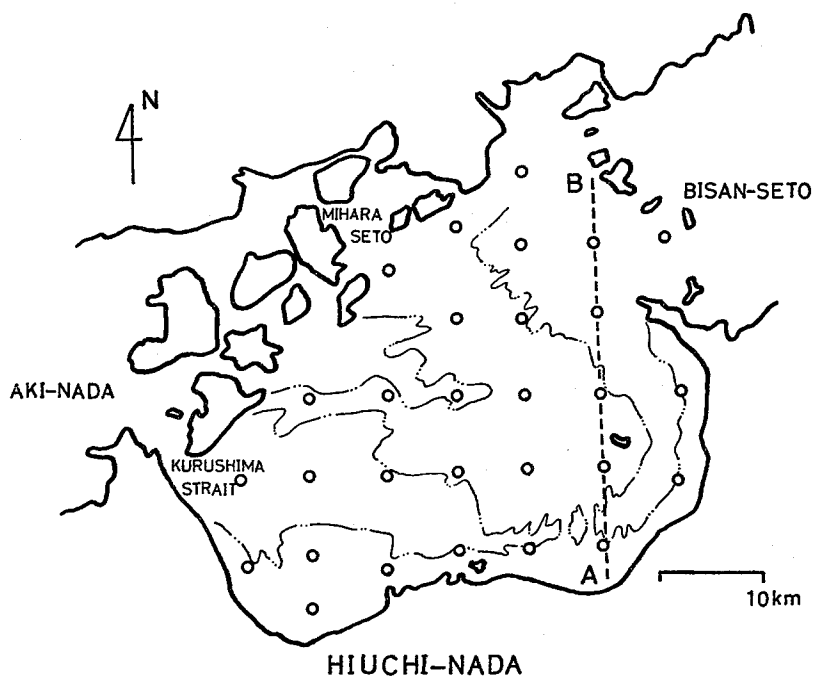


Fig. 1: The topography of Hiuchi-nada and locations (open circles) of the salinity observation.

bolatory at 28 stations, which are indicated by open circles in Fig. 1. Salinity was measured at 0, 2, 5, 10, 15, 20, 30 m depth and bottom. The horizontal distributions of the depth-averaged salinity in Aug. and Dec. are shown in Figs. 2 and 3, respectively.



In Fig. 2, some remarkable features of the distribution in Aug. can be seen: There are a high salinity water in the vicinity of Kurushima Strait (southwestern part of Hiuchi-nada) and low salinity waters in the vicinity of Mihara-seto (northwestern part) and in Bisan-seto, which are the features near the open boundaries. The remarkable features in the interior are as follows; i) a high salinity water in Kurushima Strait penetrates to the central part, ii) a low salinity water in the northwestern part penetrates to the central part, iii) there is a relatively high salinity water compared with the surroundings in the southeastern part as is shown by closed contours of salinity. Judging from these features concerning the salinity distribution in the interior, Hiuchi-nada seems to be divided into the above three regions. Since the similar features of the salinity distribution is detected in June 1972, the features of salinity distribution mentioned above may be common in summer. The salinity distribution in a vertical section along the line AB in Fig. 1 (chain line) is shown in Fig. 4. It suggests that the relatively high salinity water in the southeastern part should result from upwelling of high salinity waters from lower layers.

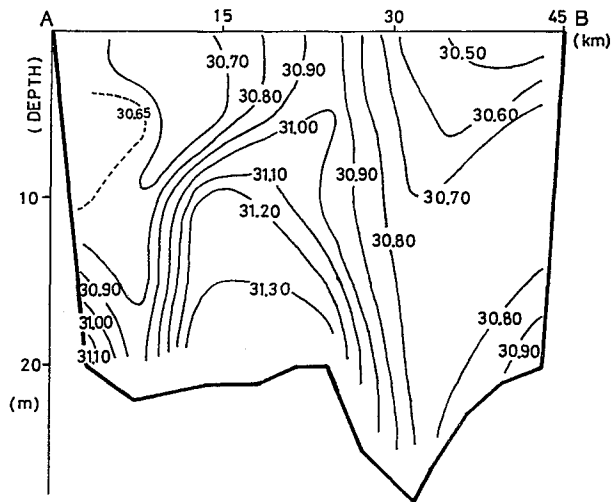


Fig. 4: The salinity distribution in a vertical section along the line AB (shown in Fig. 1).

From Fig. 3, remarkable features of the distribution in Dec. are as follows: There are a high salinity water in the vicinity of Kurushima Strait and a low salinity water in Bisan-seto, which are similar to the features near the open boundaries in summer. In the interior, salinity gradually decreases from Kurushima Strait to Bisan-seto. It should be noticed that there is no relatively high salinity water in the southeastern part. (It appears in summer.) The distribution in Dec. is simple compared with that in Aug., and is considered to be horizontal one-dimensional. Similar features are also observed in Jan. 1974 during the cruise KT 74-1 of the Tansei Maru, and they may be considered to be common features in winter.

Accordingly the patterns of salinity distributions shown in Figs. 2 and 3 may be regarded as quasi steady patterns in summer and winter, respectively, and it is suggested that the fundamental mechanisms governing salinity distributions (and/or material transport) in

summer and in winter might be different from each other.

3. Model

The horizontal two-dimensional dispersion equation developed by AK is used in order to analyze the observed horizontal distributions of salinity numerically. Since the horizontal distributions of the depth-averaged salinity in summer and winter (Figs. 2 and 3) may be considered to be quasi steady, it is reasonable to use the time-averaged dispersion equation given by AK;

$$\bar{U}_{\sigma i} \left\langle \frac{\partial \bar{S}}{\partial X_i} \right\rangle + \left\langle U_{Ti} \sin \sigma t_i \frac{\partial \bar{S}}{\partial X_i} \right\rangle = \frac{\partial}{\partial X_i} (K_H \left\langle \frac{\partial \bar{S}}{\partial X_i} \right\rangle) + \frac{\partial}{\partial X_i} \left(\left\langle E_{ij} \frac{\partial \bar{S}}{\partial X_j} \right\rangle \right), \quad (1)$$

where overbars denote the averages across the depth and brackets the time means over the present time scale (a few days to weeks). In Eq. (1), the notation of Cartesian tensor with usual summation convention is used. X_i ($i = 1, 2$) is a horizontal coordinate. $\bar{U}_{\sigma i}(X_i)$ and $\bar{U}_{Ti}(X_i)$ are components of vertically averaged velocities of a steady current and a tidal current with frequency σ , respectively, $\bar{S}(X_i)$ is vertically averaged salinity, K_H is horizontal turbulent diffusivity regarded as constant, and $E_{ij}(X_i)$ is the dispersion coefficient expressed by a tensor of the second order, which is formulated as follows;

$$E_{ij} = \frac{1}{hk_g} \int_{-h}^0 \psi_{\sigma i} \psi_{\sigma j} dz + \frac{1}{hk_g} (\sin \sigma t_i \cdot \sin \sigma t_j \int_{-h}^0 \psi_{Ti} \psi_{Tj} dz + \sin \sigma t_i \int_{-h}^0 \psi_{\sigma i} \psi_{Tj} dz), \quad (2)$$

where $\psi_{\sigma i}$ and ψ_{Ti} are

$$\psi_{\sigma i} = \int_{-h}^z U_{\sigma i} dz, \quad (3-1)$$

$$\psi_{Ti} = \int_{-h}^z U_{Ti} dz. \quad (3-2)$$

In the above equations primes denote the deviations from depth means and K_z represents vertical turbulent diffusivity.

As mentioned in the section 1, the present subjects are to study the fundamental mechanism governing material transport in Hiuchi-nada and to understand the role of the dispersion due to the tidal current which is predominant in inland seas. Therefore it may be reasonable, as a first step, to simplify the present problem as follows. The second term in the left hand side of Eq. (1), which represents the time-averaged advective effect due to the tidal current, and the unsteady component of the dispersion term (the second term) in the right hand side are neglected. The former seems to be small compared to the first term in the left hand side of Eq. (1) in the interior of Hiuchi-nada, because the phase difference between the tidal current and salinity is often found to be nearly $\pi/2$ (radian) from the observation except in the neighborhood of straits. The latter is less than the steady component and/or is at most the same order as described in AK. Also is the first term in the right hand side of Eq. (1) neglected, because horizontal turbulent diffusivity K_H is, in general, much smaller than the dispersion coefficient E_{ij} ^{1)~4)}.

Under the above simplification which does not lose the effect of the dispersion in material transport, Eq. (1) is rewritten as

$$\bar{U}_{\sigma i} \left\langle \frac{\partial \bar{S}}{\partial X_i} \right\rangle = \frac{\partial}{\partial X_i} (\left\langle E_{ij} \right\rangle \left\langle \frac{\partial \bar{S}}{\partial X_j} \right\rangle), \quad (4)$$

where $\langle E_{ij} \rangle$ can be written in the simplified form ;

$$\langle E_{ij} \rangle = \frac{1}{hk_z} \left(\int_{-h}^0 \psi_{oi} \psi_{oj} dz + \langle \sin \sigma t_i \cdot \sin \sigma t_j \rangle \int_{-h}^0 \psi_{Ti} \psi_{Tj} dz \right) \quad (5)$$

Using the conditions that salinity $\langle \bar{S} \rangle$ at the boundary is prescribed by the extrapolation of observed values and both a steady current \bar{U}_{cs} and dispersion coefficient $\langle E_{ij} \rangle$ are known, the horizontal distribution of $\langle \bar{S} \rangle$ in the interior is numerically calculated from Eq. (4). The known functions \bar{U}_{cs} and $\langle E_{ij} \rangle$ in the present calculation are decided as follows. Current measurement was carried out at 42 stations (the starting points of the arrows in Fig. 5) in Hiuchi-nada by the Sixth Regional Maritime Safety Headquarters⁶⁾ from July 25th to Aug. 8th, 1973. The tidal ellipse of the M_2 current obtained from the measurement at a depth of 5 m over a day is shown in Fig. 5. The M_2 current is the dominant current in Hiuchi-nada. The tidally-induced residual current (or mean flow) was obtained by averaging the velocity over a cycle of the M_2 tide, which is shown in Fig. 6. Since it is well

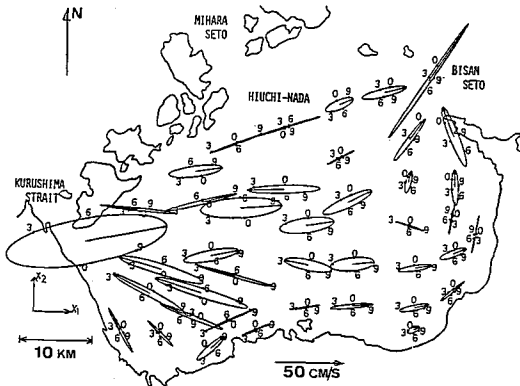


Fig. 5: Tidal ellipses of the observed M_2 current at 5 m depth. The number on the ellipses denotes the tidal phase (from The Sixth Regional Maritime Safety Headquarters, 1973).

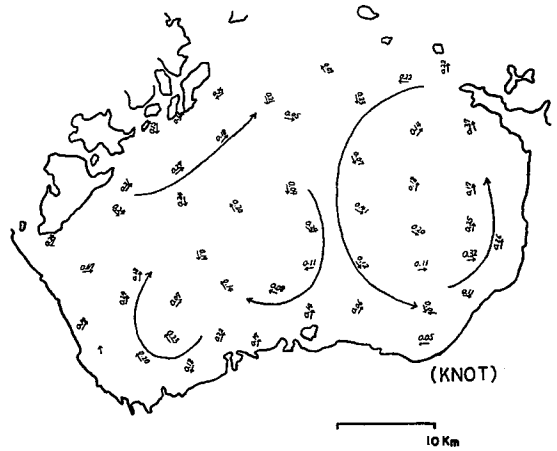


Fig. 6: The tidally-induced residual current obtained from the current measurement (from The Sixth Regional Maritime Safety Headquarters, 1973).

known that steady currents in inland seas where a tidal current is predominant mainly consist of the tidally-induced residual current⁷⁾, the obtained residual current can be regarded as a steady current and/or the most important element of a steady current. Therefore the obtained residual current (or mean flow) in Fig. 6 is used as a steady current in the present calculation of $\langle \bar{S} \rangle$.

The velocity of the residual current in Fig. 6 is much smaller than that of the M_2 current (Fig. 5). Therefore the time-averaged dispersion coefficient $\langle E_{ij} \rangle$ may be considered to be mainly due to the M_2 current. The time-averaged dispersion coefficient $\langle E_{ij} \rangle$ due to the M_2 current in Hiuchi-nada has been already evaluated from Eq. (5) by AK. The

distributions of the diagonal components $\langle E_{11} \rangle$ and $\langle E_{22} \rangle$ evaluated by AK are shown in Figs. 7 and 8, respectively, where $\langle E_{11} \rangle$ and $\langle E_{22} \rangle$ represent an east-west and a north-south component of $\langle E_{ij} \rangle$, respectively. Though the value of $\langle E_{ij} \rangle$ is an approximate one, Yuasa and Hayakawa (1980)⁸⁾ showed similar results to AK's by hydraulic experiments.

The time-averaged dispersion coefficient $\langle E_{ij} \rangle$ evaluated by AK is, therefore, used as $\langle E_{ij} \rangle$ in the present calculation.

In numerical calculations of salinity $\langle \bar{S} \rangle$, the $2.5 \text{ km} \times 2.5 \text{ km}$ finite-difference grid is used. The values of \bar{U}_{ot} and $\langle E_{ij} \rangle$ at each grid point are given by means of interpolation and/or extrapolation of the values at their known stations.

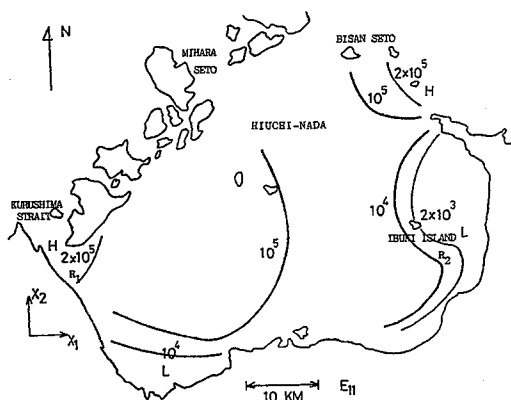


Fig. 7: The distribution of the diagonal component (an eastwest component) $\langle E_{11} \rangle$ (cm^2/s) of $\langle E_{ij} \rangle$ due to the M_2 current. (from AK, 1983).

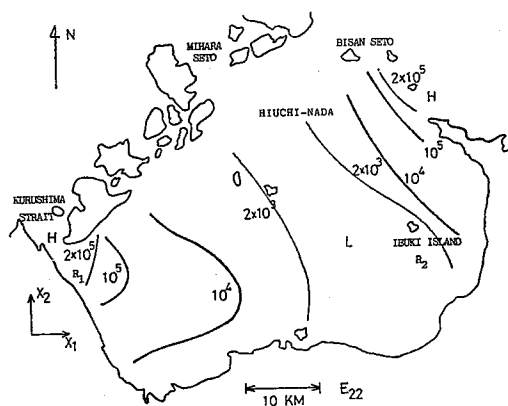


Fig. 8: The distribution of the diagonal component (a northsouth component) $\langle E_{22} \rangle$ (cm^2/s) of $\langle E_{ij} \rangle$ due to the M_2 current (from AK, 1983).

4. Results

(a) In summer

The calculated distribution of salinity $\langle \bar{S} \rangle$ in summer is shown in Fig. 9. Some remarkable features of the observed salinity distribution in summer can be seen in Fig. 9. Both a high salinity water in the vicinity of Kurushima Strait and a low salinity water in the northwestern part penetrate to the central part. The calculated distribution considerably resembles the observed distribution, judging from a large view point. The relatively high salinity water in the southeastern part, however, does not appear in the calculated distribution. The calculated distribution in the subsidiary case that $\langle E_{ij} \rangle$ is uniformly $5 \times 10^5 \text{ cm}^2/\text{s}$ all over the region is shown in Fig. 10. It is also seen in Fig. 10 that a high salinity water penetrates from Kurushima Strait to the central part. But the other remarkable features of the observed distribution are not seen. According to the other subsidiary calculation where $\langle E_{ij} \rangle$ is uniformly $10^4 \text{ cm}^2/\text{s}$, the penetration of a low salinity water from the northwestern part to the central part appears, while there is no penetration of a

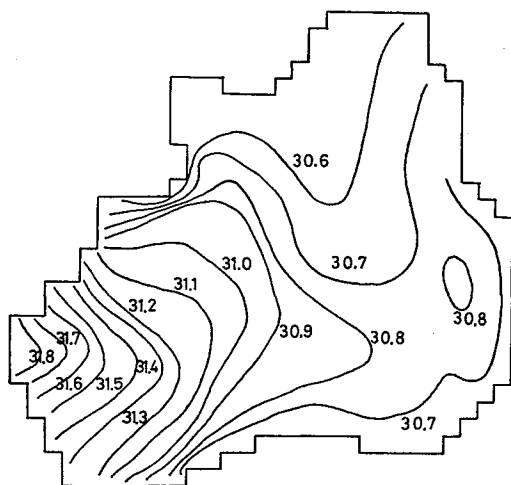


Fig. 9: The calculated distribution of salinity $\langle \bar{S} \rangle$ (%) in summer, where $\langle E_{tj} \rangle$ due to the M_2 current is used.

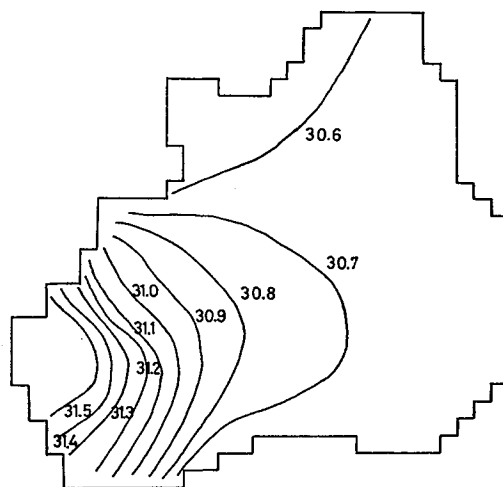


Fig. 10: The calculated distribution of salinity $\langle \bar{S} \rangle$ (%) in the case that $\langle E_{tj} \rangle$ is uniformly $5 \times 10^5 \text{ cm}^2/\text{s}$ all over the region (summer).

high salinity water from Kurushima Strait to the central part. These results mean that the dispersion coefficients larger than or equal to $10^5 \text{ cm}^2/\text{s}$ in the southwestern part and equal to about $10^4 \text{ cm}^2/\text{s}$ in the northern part are necessary to obtain the remarkable features of the observed distribution. Therefore the calculated distribution using the dispersion coefficient due to the M_2 current may be most fitting for the observed distribution. It may be due to the present model why the relatively high salinity water in the southeastern part does not appear in the calculation, because the relatively high salinity water may result from upwelling of high salinity waters from lower layers the effect of which can not be taken into account in the present model.

Accordingly the observed horizontal distribution of salinity in summer might be mainly decided by advection due to a steady current and the dispersion due to the M_2 current.

(b) In winter

The calculated distribution of salinity $\langle \bar{S} \rangle$ in winter is shown in Fig. 11, where $\langle E_{tj} \rangle$ due to the M_2 current is used. It is apparently different from the observed distribution in winter. In Fig. 11, there appear penetrations of both a high salinity water from Kurushima Strait and a low salinity water from the northern part to the central part, which are the features in summer. The calculated distribution in the case that the dispersion coefficient $\langle E_{tj} \rangle$ is uniformly $10^6 \text{ cm}^2/\text{s}$ is shown in Fig. 12. It is seen in Fig. 12 that salinity gradually decreases from Kurushima Strait to Bisan-seto. This is the remarkable feature of the observed distribution in winter. Such a result is also obtained in the subsidiary calculation where $\langle E_{tj} \rangle$ is uniformly $10^7 \text{ cm}^2/\text{s}$. These remarks mean that the dispersion coefficients of about 10^6 and/or about $10^7 \text{ cm}^2/\text{s}$ all over the region are necessary to obtain the

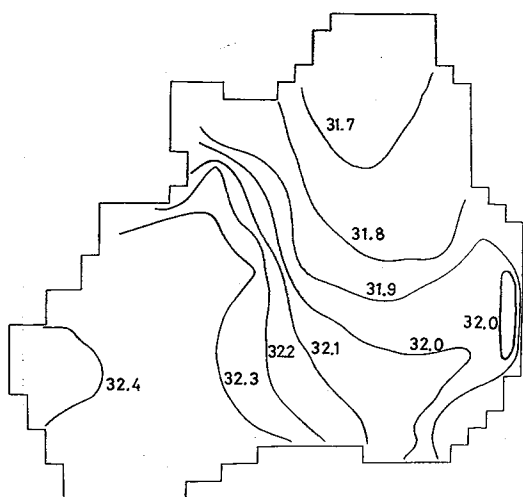


Fig. 11 : The calculated distribution of salinity $\langle \bar{S} \rangle$ (‰) in winter, $\langle E_{tj} \rangle$ due to the M_2 current is used.

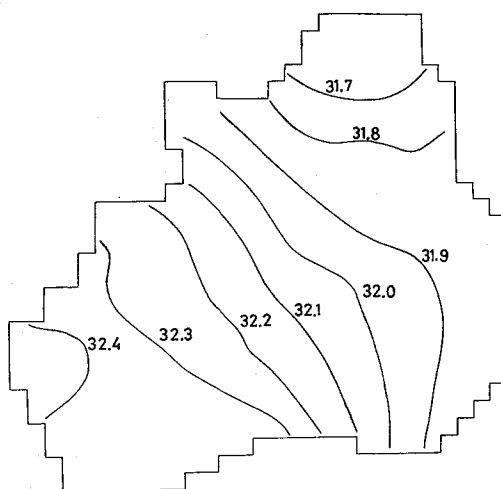


Fig. 12 : The calculated distribution of salinity $\langle \bar{S} \rangle$ (‰) in the case that $\langle E_{tj} \rangle$ is uniformly 10^6 cm²/s all over the region (winter).

features of the observed distribution in winter. In such cases the effect of advection due to a steady current in the salinity distribution is small compared to that of the dispersion, because the ratio of advection to the dispersion is considerably smaller than 1 almost all over the region.

The dispersion coefficient is inversely proportional to vertical turbulent diffusivity. It is said that the vertical turbulent diffusivity in inland seas ranges widely from a few cm²/s to a few hundred cm²/s⁹⁾. The vertical turbulent diffusivity is taken to be 50 cm²/s in AK. Even if the vertical turbulent diffusivity is taken to be less by 1 order than that in AK, the value of the dispersion coefficient $\langle E_{tj} \rangle$ due to the M_2 current becomes only a few times of the present value, because the diffusion time becomes larger than the period of the M_2 current. Therefore it is unthinkable that the dispersion coefficient due to the M_2 current becomes larger than or equal to 10^6 cm²/s all over the region, so far as the velocity of the M_2 current does not become several times of the observed velocity. Accordingly the dispersion coefficient governing the observed distribution of salinity in winter might be not due to the M_2 current: The horizontal distribution of salinity in winter (and/or material transport in winter) might be governed mainly by the dispersion alone the coefficient of which is larger than or equal to 10^6 cm²/s all over the region. (Discussions concerning this point are made in the next section.)

5. Summary and discussions

The fundamental mechanism governing the horizontal transport of matter such as salinity in Hiuchi-nada and the role of the dispersion due to the tidal current are investigated. The observed distributions of salinity in summer and winter are analyzed numerically by means of the horizontal two-dimensional dispersion model.

The following is concluded. In summer the observed distribution of salinity might be governed by both advection due to a steady current and the dispersion due to the M_2 current. The detail of the salinity distribution depends on the ratio of the advection to the dispersion. In winter the observed distribution might be governed mainly by the dispersion alone which is not due to the M_2 current. The dispersion coefficient is larger than or equal to $10^6 \text{ cm}^2/\text{s}$ all over the region. (This is far larger than that due to the M_2 current.)

In the calculated distribution of salinity in summer, the relatively high salinity water in the southeastern part does not appear. This means that, in order to investigate more exactly, it is necessary to take the effect of vertical flow into account by parameterizing.

The cause of the dispersion far larger than that due to the M_2 current in winter is unknown. It is showed that the overturning of density takes place in a considerably large part of Hiuchi-nada in a winter season⁵⁾: In a winter season, occurrence of this phenomenon in inland seas has been pointed out by many scientists. This unstable stratification induces the vertical convection. Such a vertical convection may be considered to be one of the most possible factors causing the dispersion larger than that due to the M_2 current in winter. It will be a future problem to evaluate the dispersion induced by the vertical convection.

Aknowledgements

The author wishes to express his thanks to Prof. H. Kunishi of the Geophysical Institute of Kyoto University for his discussions. The author is also grateful to the Nansei Fisheries Research Laboratory for the offer of data used in the present study. The numerical calculation were carried out in Data Processing Center of Kyoto University. A part of this study was supported by Scientific Research Fund No. 59740200 in 1984 from the Ministry of Education.

References

- 1) T. Awaji, H. kunishi : J. Oceanogr. Soc. Japan, 39, 1 (1983)
- 2) K.F. Bowden : J. Fluid Mech., 21, 83 (1965) .
- 3) A. Okubo : Int. J. Oceanol. Limnol., 1, 194 (1967) .
- 4) H.B. Fisher : J. Fluid Mech., 53, 672 (1972)
- 5) N. Imasato, H. Kunishi, H. Takeoka, H. Yoshioka, T. Yanagi, T. Awaji, S. Endoh : Bull. Coast. Oceanogr., 15, 138 (1978)
- 6) The Sixth Regional Maritime Safety Headquarters : Japan Oceanographic Data Center No. 28, p. 16 (1973)
- 7) K.T. Tee : J. Mar. Res., 34, 603 (1976)
- 8) I. Yuasa, N. Hayakawa : Rep. Govern. Industr. Res., Chugoku, 10, 19 (1988)
- 9) H.B. Fisher : Ann. Rev. Fluid Mech., 8, 107 (1976)